Performance of Pulse-Position Modulation on Measured Non-Directed Indoor Infrared Channels

Malik D. Audeh, Joseph M. Kahn, and John R. Barry

***Abstract*—We examine the performance of pulse-position modulation (PPM) on measured channels with intersymbol interference (ISI). We summarize the bit-error-rate performance of unequalized systems and review the performance of maximum-likelihood sequence detection (MLSD) for PPM over ISI channels with additive white Gaussian noise. We evaluate the performance of PPM links over 46 experimentally measured indoor infrared channels. Detailed results are presented for 2, 4, 8, and 16-PPM at bit rates of 10 Mb/s and 30 Mb/s, and these techniques are compared to on–off keying. Our results show that when MLSD is employed, 16-PPM provides the best average-power efficiency among the modulation techniques considered in this study.**

I. Introduction

NON-DIRECTED infrared (IR) radiation [1]–[3] has been shown to be a viable alternative to radio for wireless indoor communication. Many applications of non-directed IR links require high average-power efficiency to minimize ocular hazards and power consumption. We consider L-pulse position modulation (L-PPM) a technique that yields an average-power efficiency improvement with increasing order L. However, in high-speed (>10 Mb/s) indoor IR systems, we must consider the effects of intersymbol interference (ISI), resulting from reflections off floors, walls, and room objects.

The channel and noise models we consider have been discussed in detail in [2]–[4]. In order to obtain a high SNR, practical non-directed systems employing intensity modulation with direct detection (IM/DD) use photodetectors with large areas, which result in optically incoherent reception without multipath fading. However, we do observe multipath distortion, which is characterized by a linear, time-invariant impulse response $h(t)$ that changes only when the detector is moved by distances on the order of tens of centimeters [3]. In IM, the transmitted signal $X(t)$ is an instantaneous optical power. The received photocurrent $Z(t)$ is the integral of the received optical power over the detector surface, multiplied by the photodetector responsivity R.

Paper approved by P. T. Mathiopoulos, the Editor for Wireless Personal Communications of the IEEE Communications Society. Manuscript received October 4, 1994; revised March 15, 1995, September 15, 1995, and October 24, 1995. This paper was presented in part at ICC'94, New Orleans, LA, May 1994, and ICC'95, Seattle, WA, June 1995. This work was supported by National Science Foundation Grant ECS-9408957, National Science Foundation Grant NCR-9308968, Hewlett-Packard, and a National Science Foundation Graduate Fellowship.

M. D. Audeh was with the Department of Electrical Engineering and Computer Sciences, University of California, Berkeley, CA 94720 USA. He is now with Telesis Technologies Laboratory, San Ramon, CA 94583 USA.

J. M. Kahn is with the Department of Electrical Engineering and Computer Sciences, University of California, Berkeley, CA 94720 USA.

J. R. Barry is with the Department of Electrical and Computer Engineering, Georgia Institute of Technology, Atlanta, GA 30332 USA.

Publisher Item Identifier S 0090-6778(96)04354-1.

The optical IM/DD channel is normally modeled by a signal-dependent, Poisson-rate, photon-counting model. Due to the intense ambient light in indoor environments, a wireless indoor IR channel corresponds to the background-limited, high-photon-rate case. Therefore, we can neglect the shot noise caused by the signal and model the ambient-induced shot noise as a Gaussian process, which is known to be highly accurate for high-density shot noise [5]. Since the SNR of practical receivers is limited by the effects of ambient light, we do not consider the use of an avalanche photodiode, which would only decrease the receiver SNR [2].

Our channel model for IM/DD can be summarized by $Z(t) = RX(t) \otimes h(t) + N(t)$ [4]. We emphasize that our treatment of the noise $N(t)$ as Gaussian and signal-independent simplifies calculation of the error probability without any significant loss of accuracy. This channel model is similar to a standard linear, baseband channel. In particular, the receiver electrical SNR is proportional to $|X(t)|^2$, as in conventional electrical and radio systems. However, IM/DD IR links differ from conventional systems in two respects [2], [3]. First, $X(t)$ cannot be negative, since it describes an optical power. Second, the average transmitted power constraint is given by

$$P_t = \lim_{t \to \infty} \frac{1}{2T} \int_{-T}^{T} X(t)\, dt. \tag{1}$$

For a given average optical power P_t, the receiver SNR can be improved by transmitting a wave form $X(t)$ having a high peak-to-average ratio, such as L-PPM [2]. We note that the optical path loss of the channel is $H(0) = \int_{-\infty}^{\infty} h(t)\, dt$, and the received optical power is $P = H(0)P_t$.

II. L-PPM Systems

A. Unequalized Systems

Figure 1(a) displays the block diagram of an L-PPM transmitter. Independent, identically distributed (i.i.d.) input bits a_j enter a block coder of rate $(\log_2 L)/L$, which produces a length-L symbol vector having one unit chip value and $L-1$ zero chip values. The chip sequence b_k, scaled by the peak optical power LP_t, drives the transmitter filter $p(t)$, a rectangular pulse of unit magnitude and duration T/L. This results in the transmission of an optical signal $X(t)$ over the multipath channel $h(t)$, which is assumed to be fixed, positive, and have finite duration. The additive white Gaussian noise $N(t)$ has double-sided power spectral density N_0.

The unequalized receiver, designed to perform symbol-by-symbol ML detection in the absence of ISI, is shown in Fig. 1(b). This receiver employs a unit-energy filter matched

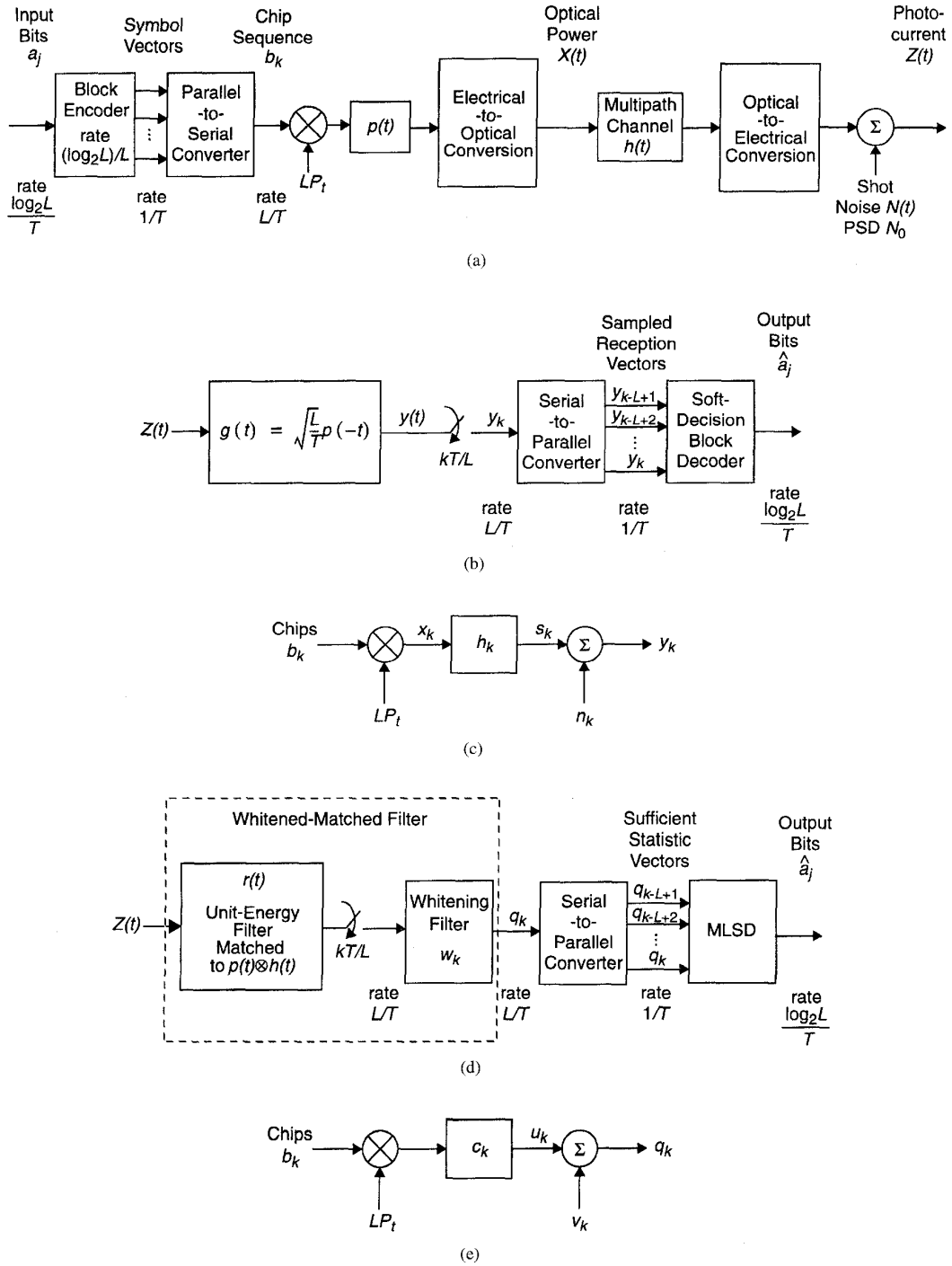

Fig. 1. (a) Block diagram of L-PPM transmission over a multipath channel. The electrical signal $Z(t)$ is input to the receiver. (b) Block diagram of unequalized L-PPM receiver. The soft block decoder chooses the received symbol based on the largest of the received samples $y_{k-L+1}, \cdots, y_k$, and yields the corresponding bit sequence. (c) Equivalent discrete-time block diagram of unequalized L-PPM system sampled at the chip rate L/T. (d) Block diagram of L-PPM receiver with whitened-matched filter followed by MLSD. (e) Discrete-equivalent model of L-PPM system prior to MLSD, sampled at the chip rate L/T.

to $p(t)$, followed by a chip-rate sampler. We can simplify the system that combines Fig. 1(a) and (b) by converting to an equivalent discrete-time model sampled at the chip rate L/T, as shown in Fig. 1(c). We define the discrete-time impulse response $h_k = p(t) \otimes h(t) \otimes g(t)|_{t=kT/L}$. The receiver makes decisions based on samples of the form $y_k = s_k + n_k$, where the signal samples s_k are derived from the chip sequence $b_k \in \{0, 1\}$ by the convolution $s_k = LP_t b_k \otimes h_k$. We note that this convolution causes each nonzero transmitted chip to interfere with samples within the same PPM symbol (intrasymbol interference), and also within adjoining PPM symbols (intersymbol interference). We refer to these two

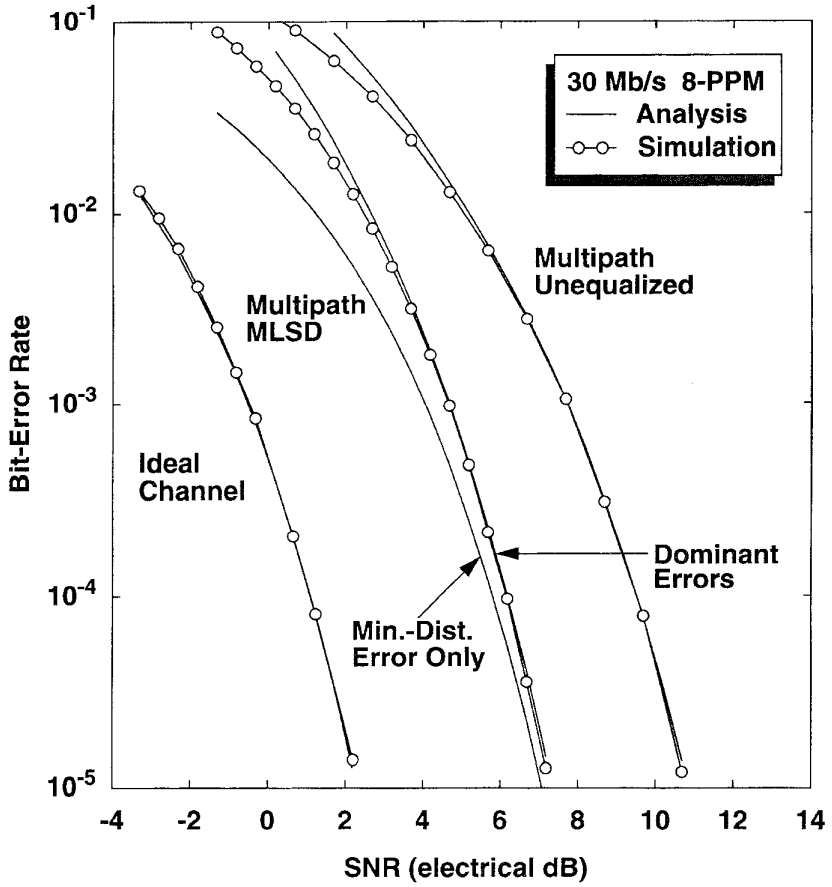

Fig. 2. BER versus SNR for 30 Mb/s, 8-PPM system, illustrating agreement between results of theory and Monte-Carlo simulation for a typical multipath channel in the shadowed diffuse configuration.

effects collectively as ISI. The noise samples n_k are i.i.d. Gaussian random variables with zero mean and variance N_0. We emphasize that n_k and s_k are independent, in contrast to the case of a photon-counting detector for PPM, which has been analyzed previously [6]. This receiver makes symbol decisions based on which is the largest of each L-length block of samples $y_{k-L+1}, \cdots, y_k$.

To illustrate the calculation of the bit-error rate (BER) for an unequalized PPM system with ISI, we assume that symbol 1 (corresponding to a chip sequence b_k of a single one followed by $L-1$ zeros) was transmitted and we assume $k = L$ [see Fig. 1(b)]. Considering the L samples $y_1, \cdots, y_L$, the probability of bit error can be well-approximated at high SNR by the following union bound:

$$P[\text{bit error}|\text{transmit symbol 1}] \approx \frac{L/2}{L-1}\left[Q\left(\frac{s_1 - s_2}{\sqrt{2N_0}}\right) + \cdots + Q\left(\frac{s_1 - s_L}{\sqrt{2N_0}}\right)\right]. \quad (2)$$

The factor $(L/2)/(L-1)$ represents the average number of bit errors per symbol error. To obtain the BER for random input data, we average over all L possible desired symbols, and over all possible interfering symbol sequences (which constitute a finite set, as $h(t)$ is finite-duration).

B. Systems with MLSD

Following [2], the MLSD receiver [see Fig. 1(d)] employs a whitened-matched filter (WMF) [7], which consists of a unit-energy continuous-time matched filter $r(t)$, followed by a discrete-time unit-energy noise-whitening filter w_k. The WMF output sequence q_k represents a sufficient statistic for optimal detection. We simplify the continuous-time realization of Fig. 1(a) and (d) into the discrete-equivalent model shown in Fig. 1(e). We define the discrete-time impulse response $c_k = [p(t) \otimes h(t) \otimes r(t)|_{t=kT/L}] \otimes w_k$. The received samples are $q_k = u_k + v_k$, where the noise samples v_k are i.i.d. zero-mean Gaussian random variables with variance N_0.

It is well-known that the optimum detector for pulse-amplitude modulation (PAM) with ISI in additive white Gaussian noise is MLSD [7], which can be implemented using the Viterbi algorithm (VA) when the signal generator can be modeled as a finite-state machine driven by a white input sequence. In a PPM system, the input chip sequence $b_k \in \{0, 1\}$ can be viewed as a PAM signal. Accordingly, the MLSD for this signal [2] chooses an estimate of the sequence b_k to minimize the sum over the entire reception of the per-chip branch metric $|q_k - u_k|^2$. As the sequence b_k is not i.i.d. (in fact, it is cyclostationary), however, the MLSD for PPM cannot be implemented using a chip-by-chip VA. Thus, we

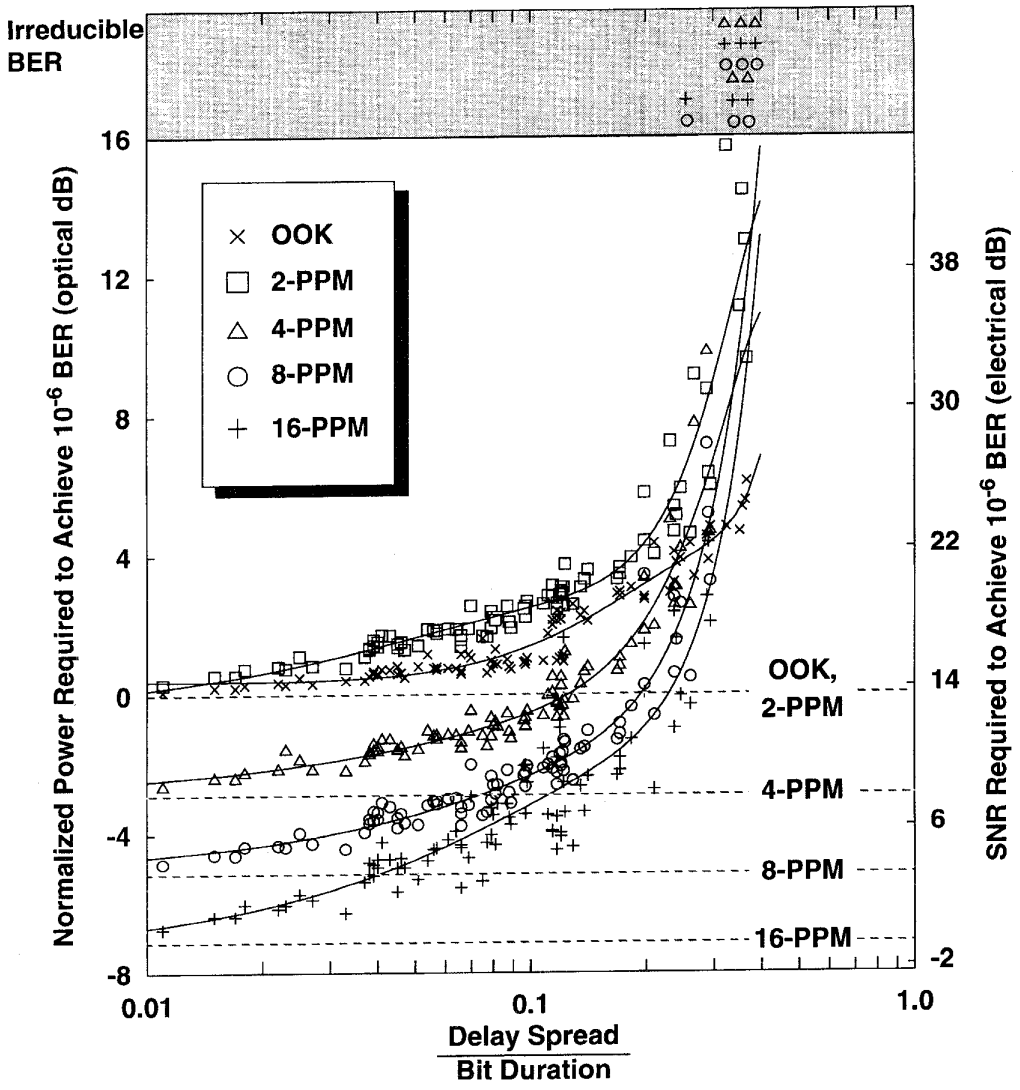

(a)

Fig. 3. (a) Normalized optical average power (left axis) and electrical SNR (right axis) required to achieve 10^{-6} BER versus delay spread divided by bit duration with five different modulation schemes for unequalized systems. These graphs include all four link configurations at 10 and 30 Mb/s. The horizontal dashed lines represent performance over an ideal channel. In the region of irreducible bit-error rate (infinite penalty), the different symbols have been vertically separated to enhance visibility. The solid lines represent fourth-order least-squares polynomial fits to the data for each modulation scheme.

view the signal as a sequence of L-length PPM symbol vectors that pass through a multiple-input, multiple-output channel [2]. Since this symbol sequence is i.i.d., the MLSD can be implemented using a symbol-by-symbol VA that employs a per-branch metric given by $\Sigma_{k=0}^{L-1} |q_k - u_k|^2$, provided that the duration of c_k is finite.

The probability of bit error for MLSD of PPM can be well-approximated at high SNR by [7]

$$\Pr(\text{bit error}) \approx \frac{L/2}{L-1} Q\left(\frac{d_{\min}}{2\sqrt{N_0}}\right) \tag{3}$$

$$d_{\min}^2 = \min_{\{e_k\}} \sum_{k=0}^{\infty} \left| \sum_{m=0}^{\infty} c_m e_{k-m} \right|^2. \tag{4}$$

The minimization in (4) is performed over all nonzero error sequences $\{e_k\}$ starting at time zero, i.e., over all $e_k = b_k - b'_k$ where b_k and b'_k are valid PPM chip sequences.

III. Performance Results on Measured Channels

This section quantifies the performance of the PPM systems of Section II in transmitting over a collection of 46 experimentally measured channels [4]. Non-directed IR channels may be classified as either *line-of-sight* (LOS), which rely upon the existence of an unobstructed path between transmitter and receiver, or *diffuse*, which alleviate the need for a LOS path by relying on reflections from a large diffuse reflector. We consider four channel configurations: unshadowed LOS, unshadowed diffuse, shadowed LOS, and shadowed diffuse (see Fig. 2 of [4]).

Figure 2 presents the BER versus electrical SNR for an 8-PPM system transmitting at a bit rate of 30 Mb/s over both an ideal channel $h(t) = \delta(t)$ and a typical shadowed diffuse multipath channel. In order to facilitate comparison of average-power efficiency, we define the electrical SNR as

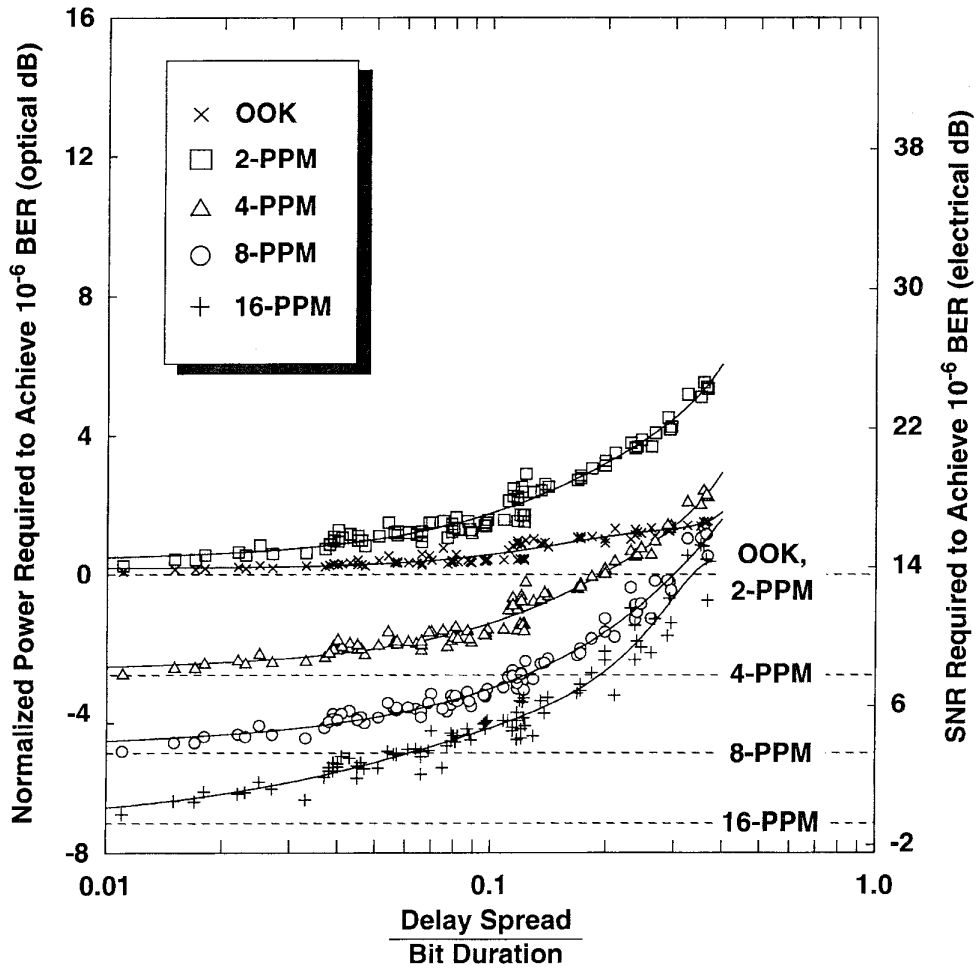

(b)

Fig. 3. (*Continued.*) (b) Normalized optical average power (left axis) and electrical SNR (right axis) required to achieve 10^{-6} BER versus delay spread divided by bit duration with five different modulation schemes for systems employing MLSD. These graphs include all four link configurations at 10 and 30 Mb/s. The horizontal dashed lines represent performance over an ideal channel. In the region of irreducible bit-error rate (infinite penalty), the different symbols have been vertically separated to enhance visibility. The solid lines represent fourth-order least-squares polynomial fits to the data for each modulation scheme.

R^2P^2/R_bN_0, where R_b is the system bit rate (note that this is $1/L$ times the usual definition of SNR, E_b/N_0). Fig. 2 compares results of analysis and Monte-Carlo simulation. The BER performance of MLSD is computed both by considering the union bound of all dominant error events, and by considering only the error event having the minimum distance. At moderate-to-low BER, there is excellent agreement between the BER's computed considering only the minimum-distance error event and considering all dominant error events. This agreement validates our use of (3) to compute the BER of MLSD in the remainder of this paper. Moreover, we emphasize that all analytical results shown in Fig. 2 are in agreement with the results of Monte-Carlo simulation.

In comparing the optical average-power efficiency of various modulation techniques in transmission at a given bit rate over a given multipath channel, we compare the electrical SNR required to achieve 10^{-6} BER, and also the optical power required to achieve that same BER, normalized to the power required to achieve the same BER using OOK (or 2-PPM) on an ideal channel $h(t) = \delta(t)$. A 1-dB change of optical power corresponds to a 2-dB change of electrical SNR in our IM/DD system with signal-independent noise. In previous work, it was observed that for unequalized and equalized OOK links, the impact of multipath ISI is well-correlated to the channel r.m.s. delay spread, normalized by the bit duration (see Figs. 7 and 11 of [4]).

Figure 3 compares the optical average-power (and electrical SNR) requirement for unequalized PPM (orders 2, 4, 8, and 16) and OOK links to those employing MLSD, considering all channels of all four configurations, at bit rates of 10 Mb/s and 30 Mb/s, organized according to the r.m.s. delay spread divided by the bit duration. We see that either without equalization or with MLSD, the power requirement for each technique increases nearly monotonically with increasing delay spread. We see that as the delay spread increases, the MLSD power requirement does not grow as quickly as the unequalized power requirement. Furthermore, we observe that in cases where the unequalized system incurs an irreducible BER

[see Fig. 3(a)], the MLSD power requirement is finite [see Fig. 3(b)]. If no equalization is employed, then the ordering of average-power efficiency among the modulation schemes considered depends on the channel delay spread. By contrast, when MLSD is utilized, 16-PPM consistently yields the best average-power efficiency.

IV. Conclusions

We have compared the performance of unequalized PPM and OOK links operating at 10 Mb/s and 30 Mb/s to those using MLSD, using measured responses of non-directed indoor infrared channels. MLSD offers significant improvement over unequalized systems. Even with MLSD, however, as the ratio of delay spread to bit duration increases, the advantage of any given PPM order over OOK diminishes. We have found that when the delay spread becomes higher than approximately 0.25 times the bit duration, OOK achieves performance superior to 4-PPM when MLSD is used. Similarly, with MLSD, OOK achieves performance superior to 8-PPM when the delay spread is higher than 0.35 times the bit duration.

References

[1] F. R. Gfeller and U. H. Bapst, "Wireless in-house data communication via diffuse infrared radiation," *Proc. IEEE*, vol. PROC-67, pp. 1474–1486, Nov. 1979.

[2] J. R. Barry, *Wireless Infrared Communication*. Boston, MA: Kluwer, 1994.

[3] J. M. Kahn *et al.*, "Non-directed infrared links for high-capacity wireless LANs," *IEEE Pers. Commun. Mag.*, vol. 1, no. 2, pp. 12–25, May 1994.

[4] J. M. Kahn, W. J. Krause, and J. B. Carruthers, "Experimental characterization of non-directed indoor infrared channels," *IEEE Trans. Commun.*, vol. 43, pp. 1613–1623, Feb./Mar./Apr. 1995.

[5] A. Papoulis, *Probability, Random Variables, and Stochastic Processes*. New York: McGraw-Hill, 1984.

[6] S. Karp, E. L. O'Neill, and R. M. Gagliardi, "Communication theory for the free-space optical channel," *Proc. IEEE*, vol. PROC-58, pp. 1611–1626, Oct. 1970.

[7] G. D. Forney, "Maximum-likelihood sequence estimation of digital sequences in the presence of intersymbol interference," *IEEE Trans. Inform. Theory*, vol. IT-18, pp. 363–378, May 1972.